# Temporal Airy pulses control cell poration

S. Courvoisier,[1] N. Götte,[2] B. Zielinski,[2] T. Winkler,[2] C. Sarpe,[2]
A. Senftleben,[2] L. Bonacina,[1] J. P. Wolf,[1] and T. Baumert[2]
[1]*GAP-Biophotonics, University of Geneva, ch. de Pinchat 22, 1211 Geneva 4, Switzerland*
[2]*Experimentalphysik, Universitaet Kassel, Heinr.-Plett-Straße 40, 34132 Kassel, Germany*

(Received 2 February 2016; accepted 18 April 2016; published online 24 June 2016)

We show that spectral phase shaping of fs-laser pulses can be used to optimize laser-cell membrane interactions in water environment. The energy and peak intensity thresholds required for cell poration with single pulse in the nJ range can be significantly reduced (25% reduction in energy and 88% reduction in peak intensity) by using temporal Airy pulses, controlled by positive third order dispersion, as compared to bandwidth limited pulses. Temporal Airy pulses are also effective to control the morphology of the induced pores, with prospective applications from cellular to tissue opto-surgery and transfection.  [http://dx.doi.org/10.1063/1.4948367]

Current DNA delivery techniques can be divided into two major categories: viral- and non-viral-mediated.[1] In viral transfection, the genes of interest replace viral genetic material without eliminating the ability of the virus to target specific cells and deliver the vector efficiently to the nucleus.[2] The use of viral methods has been limited so far to clinical trials and laboratory assays because of the risk of developing cellular-specific immune response and of inducing genotoxicity after insertional mutagenesis.[3–6] Electroporation was introduced as a non-viral technique for a direct entry of the DNA into the cell. It involves pulsing or cycling large gradients of the electric potential that induce transient permeability of the membrane.[7] While applicable to many systems, such harsh conditions often result in high mortality.[8] Electroporation and its successful recent improvements in transfection efficiency and cell viability are currently the most widely used physical gene-delivery methods. However, the spatial selectivity of electroporation is limited by the electrode shape and size.[9]

With the advent of short-pulse lasers in the 1990's, a new transfection technique emerged, based on laser-assisted poration of the cell membrane. Generation of a transient pore allows uptake of a vector with efficiencies up to 50%–100%.[10,11] In the case of stem cells, however, yields of only 25% have been achieved with opto-transfection.[12,13] In opto-transfection, the cell survival is related to phototoxicity. For example, direct DNA photodamage can occur, as reported for various pulse durations, wavelengths, and number of shots.[14,15] It is therefore of primary importance to optimize the laser-membrane interaction in order to increase the perforation yield while reducing long term cell damage. Very interesting results have recently been reported on the use of optimally shaped laser pulses for drilling micrometric holes in glass.[16,17] In particular, it was demonstrated that the use of third order phase control could manipulate the interaction with the substrate and lead to holes of different sizes, as small as one order of magnitude below the diffraction limit.[18] Such third order phase control leads to temporal pulse shapes that are termed Airy pulses.[19] Furthermore, it was recently shown that the volume of laser-excitation in bulk water can be controlled by such pulse shapes.[20] By using positive third order dispersion laser pulses, the area of excitation can be reduced by nearly a factor of two while the depth of the excitation reached much deeper inside the bulk water sample.

In this paper, we explore the effect of single pulse phase-shaping on cell-laser interaction for a prospective future use for poration/transfection or laser surgery. In particular, we show that optimally shaped temporal Airy pulses (TAPs) can control the poration of fixed cell membranes,

 

with variable hole sizes and even hole-less poration (small recesses and fractures), and significantly reduce the necessary intensity (by a factor 6) and energy (by 25%) for hole creation as compared to unshaped Gaussian pulses.

We investigated the influence of the femtosecond laser pulse shapes on the induced surface damages on adherent cervix cancer cell line (HeLa) on glass immersed in water. Four types of pulse shapes were selected: Bandwidth limited pulses (BWL), temporal Airy pulse (TAP) induced by a high third order dispersion of +600 000 $fs^3$ for TAP+ pulses and −600 000 $fs^3$ for TAP− pulses and linearly positively chirped pulses with a group delay dispersion (GDD) of +15 000 $fs^2$. Temporally, TAP pulses are asymmetric. TAP+ consists of a high intensity pulse followed by a train of weaker sub-pulses of decreasing intensities. Conversely, TAP− is the time reversed version with increasing intensities sub-pulses ended by the most intense pulse. The group delay dispersion parameter of GDD pulses was defined to match the average pulse duration of TAP pulses. For a more precise description of these pulse shapes, see, for example, Refs. 21 and 22.

We used a home-built spectral phase modulator[23] associated with a femtosecond laser micromachining setup as schematized in Fig. 1. Bandwidth limited linearly polarized laser pulses of 30 fs full width at half maximum (FWHM) duration are provided by an amplified Ti:Sapphire laser system at a central wavelength of 785 nm. The pulses are focused at the sample with a 40×, 0.75 NA, water immersion microscope objective (Zeiss N-Achroplan). We assumed a 0.7-$\mu$m waist at focal position as the beam radius was 50% of the objective pupil radius of our 0.75 NA objective.[24] All pulse types are additionally corrected for chromatic dispersion along the optical path (e.g., in the objective). The compensation dispersion was determined by achieving a reference BWL laser pulse at the interaction region.

Each targeted spot on the cell membrane was irradiated by a single laser pulse. The focal waist was adjusted by a piezo scanning stage at 6 $\mu$m above the confocally identified glass surface. This position corresponds approximately to the cell membrane height.

HeLa cells were seeded and cultured in incubator (5% $CO_2$ at 37 °C) on glass coverslips to form small flat colonies of approximately 100-150 $\mu$m diameter. Cells were fixed beforehand with 2% formaldehyde, 2% glutaraldehyde in phosphate buffered saline solution (PBS) and postfixed with Osmium tetroxide. Cells were stored in 2% formaldehyde, 2% glutaraldehyde in phosphate buffered saline solution (PBS) at 5 °C. The fixative solution was replaced by PBS before laser processing. Processed samples were placed back in fixative solution before being prepared for examination under scanning electron microscope (SEM).

Figure 2 shows SEM images of two sample areas with adherent HeLa cells: (a) without laser irradiation as a control and (b) after laser treatment with a shaped pulse, namely, a positive temporal Airy pulse (TAP+). The white crosses indicate the nominal positions of laser shots, the inter-shot spacing being 7.5 $\mu$m along both horizontal and vertical axis. Different damages on the cell surfaces

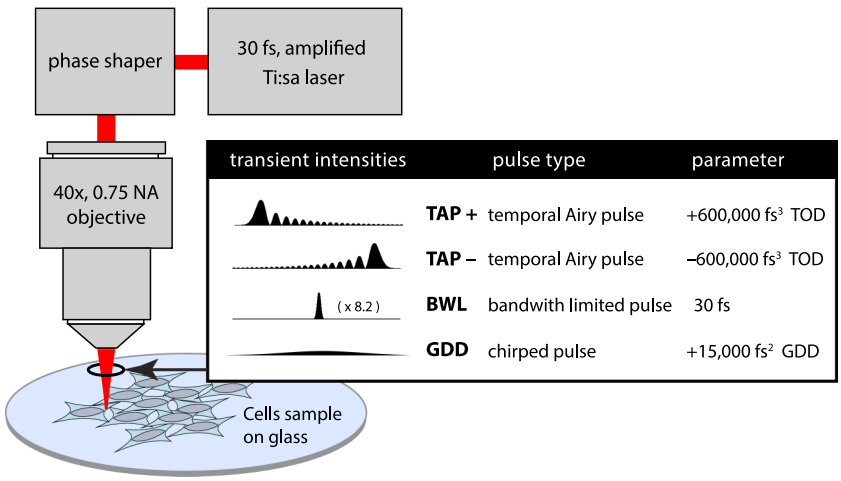


FIG. 1. Schematic of the experimental setup and illustration of the applied pulse shapes.

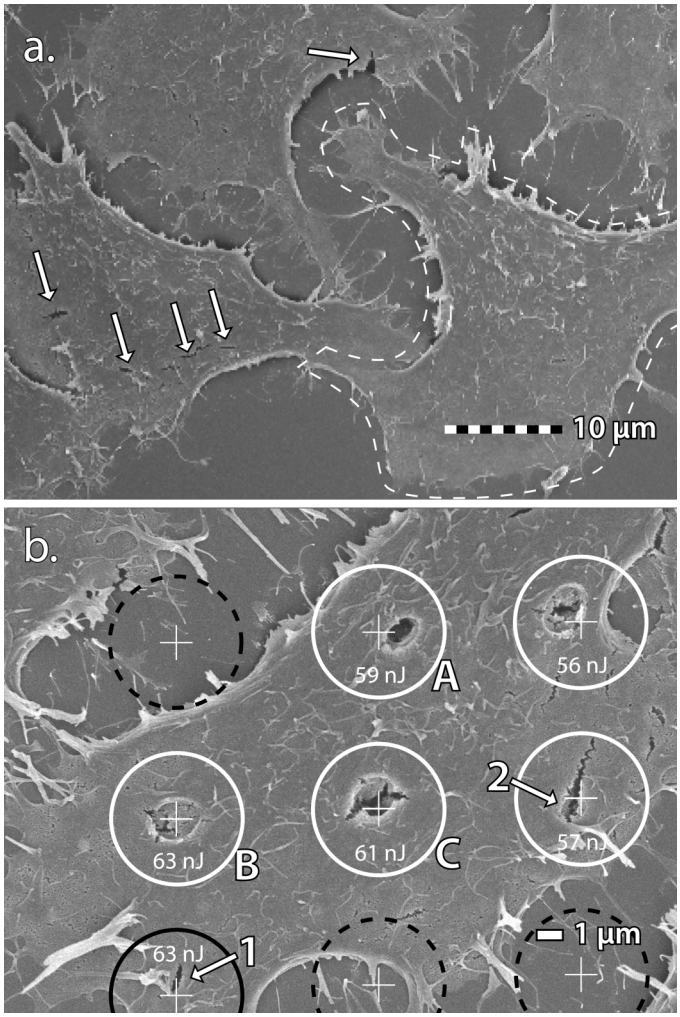


FIG. 2. SEM of dehydrated HeLa cells on glass. (a.) Unprocessed area: the dashed white outline indicates one HeLa cell. White arrows point out dehydration induced cracks. (b.) Laser processed area with TAP+: white crosses are nominal laser position; energy per pulse increases right to left from 56 nJ to 63 nJ. Solid white circles indicate successful laser-induced poration, the solid black circle indicates a failed attempt, and black dashed circles indicate attempts not accounted for.

are observed, ranging from irregular cracks to neatly shaped circular holes. Since the cells surface height is not evenly flat, part of the variability in the results arises from the laser focal plane position relative to the cell surface. To minimize this variability, we carefully selected the cell clusters to be as flat as possible with no overlapping cells and no rounded cell shape (associated with cell division[25]). In our analysis, we used the following criterion for considering an interaction: the cell material should cover more than two-third of a circular area defined by a diameter of 5 $\mu$m and centered at the expected position. Second, as beam wandering, vibrations and sample movement can lead to differences between the targeted and the actual laser position, successful laser-induced damages are validated if they co-localize with a nominal laser shot position within 2.5 $\mu$m. All the retained damages can be described as material ablation (A), circular recesses (B), or radial cracks (C), as shown in Fig. 2. Finally, each ambiguous event is visually evaluated and assigned to the relevant categories. For instance, the damage indicated with white circles is considered genuine damages, while the one pointed at by arrow 1 is not retained because the crack cannot be differentiated from a crack induced by the dehydration process necessary for SEM examination (white arrows in the non-processed area). Some damages may not be obvious, for example, arrow 2 indicates most likely a laser-induced cell-material ablation at the bottom of a crack likely induced by dehydration.

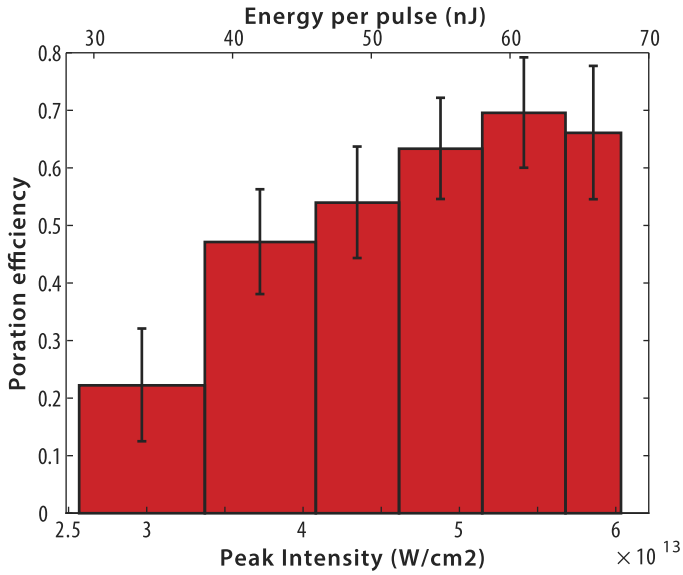


FIG. 3. Laser induced poration efficiency for TAP+ pulse shape.

Because of this ambiguity, this type of damages was not retained for further analysis. Based on these criteria, we calculated for each pulse shape the normalized poration efficiency, as the number of successful laser damage attempts divided by the total number of laser damage attempts aimed at the inner regions of cells (first criterion). Fig. 3 shows the energy (top axis) and peak intensity (bottom axis) dependence of successful damage rate plotted also in this case for the TAP+ pulse type. One can clearly observe the onset of the effect at 35 nJ (respectively, $3 \times 10^{13}$ W cm$^{-2}$) with 20% poration success. This value rapidly grows and saturates at approximately 70% efficiency starting from 55 nJ (respectively, $5 \times 10^{13}$ W cm$^{-2}$) without further evolution beyond the limits shown in the plot.

The main goal of this study is to evidence the effect of temporal shaping on poration efficiency for pulses bearing similar pulse energies and intensities. In the comprehensive Fig. 4, the results

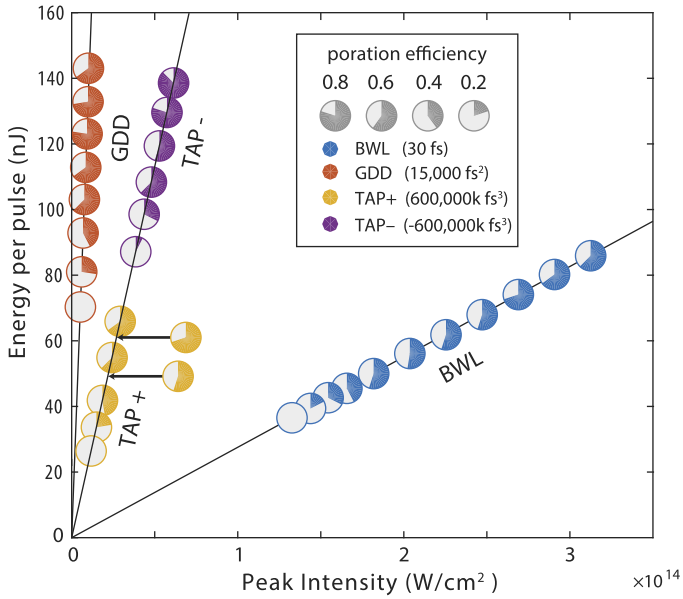


FIG. 4. Laser induced poration efficiency for the four pulse shapes as a function of the assumed peak intensity and energy for a beam waist of 0.7 $\mu$m. Here, only the relative peak intensity and its order of magnitude are relevant for the discussion.

obtained for pulses, respectively, bandwidth limited (BWL), linearly positive chirped (GDD), positive (TAP+) and negative (TAP−) temporal Airy pulses are directly compared against their energy and highest peak intensity. The different phase profiles define well-separated regions across the energy-intensity space; the diagonal arrangements are consequence of the linear dependence between these two parameters. The existence of such distinct ensembles confirms the influence of pulse phase profile on the interaction with cell membranes and the surrounding medium. Clearly, when choosing a specific temporal shape for a poration procedure, one's efforts are focused on limiting the collateral damages, which might ensue from excessive heat deposition (proportional to energy) or unwanted nonlinear interactions. In this respect, TAP+ stand out (in Fig. 4) as the most promising candidate as for comparatively smaller energy and intensity such pulses provide a poration efficiency equal or larger than all the other pulses tested. Such differences in poration efficiency in energy and peak intensity can be explained by the different temporal intensity distribution within the various pulse types. For positive cubic phase pulses (TAP+), the high intensity peak coming at early times induces multiphoton ionization ($\propto I^6$) that increases the free-electron density in water. Subsequently, the decreasing intensity train of pulses releases additional electrons by avalanche ionization. While for the negative cubic phase counterpart (TAP−), the situation is different. The electron density increases only at the trailing edge, as smaller peaks do not contribute due to the extreme nonlinear dependence involved in the process.[26]

Successively, we have globally classified the conformational aspects of the laser damages (material ablation (A), circular recesses (B), or radial cracks (C)) to unveil any correlation among pulse temporal characteristics and damage type. The results of this comprehensive analysis are reported in Fig. 5, along with typical examples from SEM of the related damage type. The given rates are relative to the number of shots where damage occurred. Note that the energy range scale for each pulse shape is independent and adjusted in order to encompass the values going from the onset of cell damage to the plateau in damage success rate, as reported for TAP+ in Fig. 3.

For radial cracks, we do not observe any statistically significant difference among pulse types throughout the energy range investigated, which might be rather related to local structural properties of cells. A feature common to all pulse types is an increase of cracks at higher energies.

For ablation and circular recess on the other hand, there exists a significant correlation with pulse type. In particular, TAP+ are systematically associated with highest ablation and lowest recess damage rate while the opposite behavior is observed for TAP−. At the intensity scale we are investigating, laser induced breakdown in water can lead to the formation of cavitation bubbles.[27]

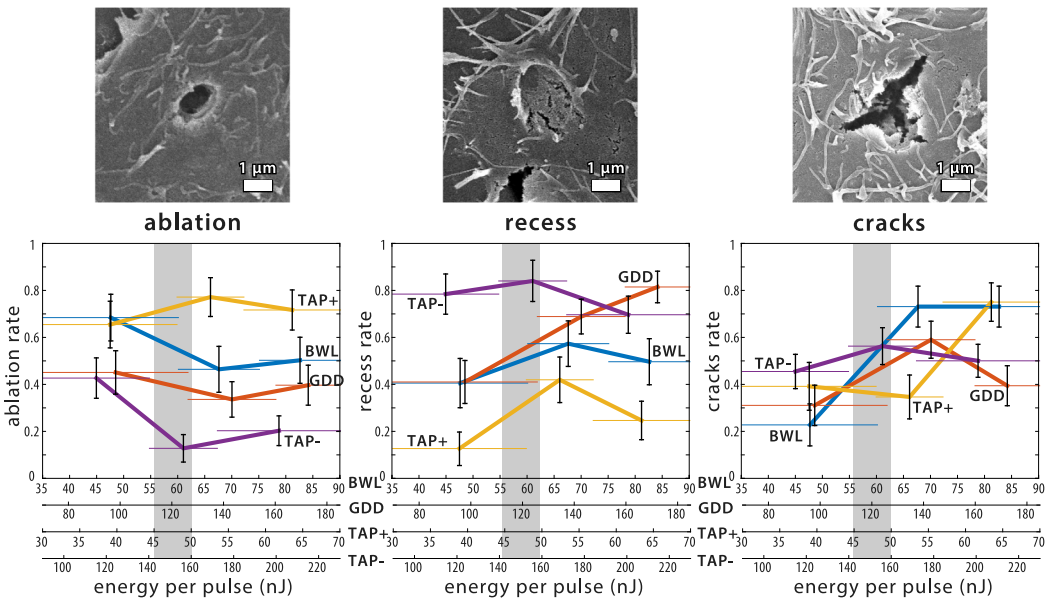


FIG. 5. Poration rate for the three non-exclusive damage types as a function of the energy per pulse.

Morphological examination of circular recesses suggests that this damage type is produced by the fast expansion of a vapor bubble produced in the water slightly above the cell membrane. These findings are probably related to the different energy ranges investigated here for the two pulse types (see x-axis scale in Fig. 5) set at a similar intensity. In fact, in previous works, it was observed that ionization threshold in water is slightly higher for TAP− compared to TAP+.[26] Bandwidth limited and temporally chirped pulses are somehow in between the two extrema (TAP+, TAP−).

In general, as mentioned before, the z-positioning is fixed relatively to the glass surface while the cell surface is not even and has a fried egg shape when adherent. Thus, the cell membrane position relatively to the glass surface ranges from 3 to 10 $\mu$m depending on the cell and the region in the cell. As all pulses types are equivalently distributed on cell samples and each data point in Fig. 5 is composed of approximately 40 successful shots, the observed averaged variation should come from the pulse type. For energy per pulse at the beginning of the damage success rate plateau (Fig. 3), one can largely modulate the interaction (i.e., damage type) by the pulse temporal profile while keeping a high damage rate with comparatively small pulse energy. This energy per pulse regime corresponds to the gray shaded area in all three graphs of Fig. 5. In these energy per pulse regions, cracks associated damages are still limited. One can argue that such holes drilled in cells may compromise cell survival. Interestingly, it was shown that large membrane laser-induced holes are, counter-intuitively, associated with a faster resealing dynamics compared to small holes, suggesting an active resealing mechanism triggered by large membrane damages.[28]

Our results can be compared to recent measurements on cell optoporation by pairs of 100 fs BWL pulses at 1 kHz from an amplified Ti:Sapphire laser.[28] The authors report successful poration and transfection with cell viability figures comparable to those obtained in pJ-level oscillator-based experiments.[14] As those measurements were performed by BWL pulses, we could expect by spectral pulse shaping similar—or better—transfection rate and increased viability thanks to the 25% reduction in energy and 88% reduction in peak intensity associated with TAP+.

We investigated the effect of phase shaping of single fs-pulses on laser-cell membrane interaction in water (poration threshold, rate, and damage morphology). In particular, we focused on TAP± (temporal Airy pulse), characterized by high positive and negative third order dispersion ($6 \times 10^5$ fs$^3$). Their performances were compared to BWL and GDD pulses. TAP+ was found to induce poration at lower intensity (88% reduction) and energy (25% reduction) than other pulse types. TAP− can also produce successful surface damage at half the intensity of BWL pulses. This intensity reduction suggests a lower phototoxicity for poration application on live cells. The second part of our analysis, focused on damage morphology, revealed that slightly above damage threshold, TAP− was found to produce recess damages, likely induced by cavitation bubble expansion, whereas TAP+ induces mostly ablation damage at the cell surface. The differences observed between pulse types could allow a better control of laser-cell interaction leading to improved methods for cell molecular intake, transfection, and sub-cellular or tissue surgery.

This work was supported by the NCCR Molecular Ultrafast Science and Technology (NCCR MUST), a research instrument of the Swiss National Science Foundation (SNSF). Similarly, we received support from the German Research Foundation (DFG) within the priority program 1327 and from Otto Braun Fund for a PhD scholarship (Thomas Winkler). We acknowledge technical assistance from Michel Moret and the technical workshop as well as Christoph Bauer and Jérôme Bosset from the bioimaging Center at the University of Geneva.

[1] N. Somia and I. M. Verma, "Gene therapy: Trials and tribulations," Nat. Rev. Genet. **1**, 91–99 (2000).
[2] P. J. Carter and R. J. Samulski, "Adeno-associated viral vectors as gene delivery vehicles (review)," Int. J. Mol. Med. **6**, 17–27 (2000).
[3] Y. Yang *et al.*, "Cellular immunity to viral antigens limits E1-deleted adenoviruses for gene therapy," Proc. Natl. Acad. Sci. U. S. A. **91**, 4407–4411 (1994).
[4] S. Hacein-Bey-Abina *et al.*, "LMO2-associated clonal T cell proliferation in two patients after gene therapy for SCID-X1," Science **302**, 415–419 (2003).
[5] F. D. Ledley, "Review nonviral gene therapy: The promise of genes as pharmaceutical products," Hum. Gene Ther. **6**, 1129–1144 (1995).
[6] L. Naldini, "Gene therapy returns to centre stage," Nature **526**(7573), 351–360 (2015).
[7] E. Neumann, M. Schaeferridder, Y. Wang, and P. H. Hofschneider, "Gene-transfer into mouse lyoma cells by electroporation in high electric-fields," EMBO J. **1**, 841–845 (1982).
[8] D. Luo and W. M. Saltzman, "Synthetic DNA delivery systems," Nat. Biotechnol. **18**, 33–37 (2000).

[9] J. L. Young and D. A. Dean, *Electroporation-Mediated Gene Delivery*, Advances in Genetics (Elsevier Ltd, 2015), Vol. 89.
[10] U. K. Tirlapur and K. König, "Targeted transfection by femtosecond laser," Nature **418**, 290–291 (2002).
[11] D. Stevenson *et al.*, "Femtosecond optical transfection of cells: Viability and efficiency," Opt. Express **14**, 7125–7133 (2006).
[12] P. Mthunzi, K. Dholakia, and F. Gunn-Moore, "Phototransfection of mammalian cells using femtosecond laser pulses: Optimization and applicability to stem cell differentiation," J. Biomed. Opt. **15**, 041507 (2010).
[13] A. Uchugonova, K. Konig, R. Bueckle, A. Isemann, and G. Tempea, "Targeted transfection of stem cells with sub-20 femtosecond laser pulses," Opt. Express **16**, 9357–9364 (2008).
[14] A. P. Rudhall, M. Antkowiak, X. Tsampoula, M. Mazilu, N. K. Metzger, F. Gunn-Moore, and K. Dholakia, "Exploring the ultrashort pulse laser parameter space for membrane permeabilisation in mammalian cells," Sci. Rep. **2**, 858 (2012).
[15] X. Kong *et al.*, "Comparative analysis of different laser systems to study cellular responses to DNA damage in mammalian cells," Nucleic Acids Res. **37**, e68 (2009).
[16] J. Hernandez-Rueda *et al.*, "Nanofabrication of tailored surface structures in dielectrics using temporally shaped femtosecond-laser pulses," ACS Appl. Mater. Interfaces **12**(7), 6613–6619 (2015).
[17] L. Englert, M. Wollenhaupt, C. Sarpe, D. Otto, and T. Baumert, "Morphology of nanoscale structures on fused silica surfaces from interaction with temporally tailored femtosecond pulses," J. Laser Appl. **24**, 1–5 (2012).
[18] L. Englert, B. Rethfeld, L. Haag, M. Wollenhaupt, and T. Baumert, "Control of ionization processes in high band gap materials via tailored femtosecond pulses," Opt. Express **15**(26), 17855 (2007).
[19] D. Abdollahpour, S. Suntsov, D. G. Papazoglou, and S. Tzortzakis, "Spatiotemporal Airy light bullets in the linear and nonlinear regimes," Phys. Rev. Lett. **105**(25), 1–4 (2010).
[20] T. Winkler *et al.*, "Probing spatial properties of electronic excitation in water after interaction with temporally shaped femtosecond laser pulses Experiments and simulations," Appl. Surf. Sci. **374**, 235–242 (2016).
[21] M. Wollenhaupt, "Control of ionization processes in high band gap materials," J. Laser Micro/Nanoeng. **4**(3), 144–151 (2009).
[22] M. Wollenhaupt, L. Englert, A. Horn, and T. Baumert, "Temporal femtosecond pulse tailoring for nanoscale laser processing of wide-bandgap materials," Proc. SPIE **7600**, 76000X (2010).
[23] J. Köhler, M. Wollenhaupt, T. Bayer, C. Sarpe, and T. Baumert, "Zeptosecond precision pulse shaping," Opt. Express **19**(12), 11638 (2011).
[24] H.-S. Chon, G. Park, S.-B. Lee, S. Yoon, J. Kim, J.-H. Lee, and K. An, "Dependence of transverse and longitudinal resolutions on incident Gaussian beam widths in the illumination part of optical scanning microscopy," J. Opt. Soc. Am. A **24**(1), 60–67 (2007).
[25] R. G. Kessel and C. Y. Shih, *Scanning Electron Microscopy in Biology* (Springer, Berlin Heidelberg, 1976), Vol. 17.
[26] C. Sarpe, J. Köhler, T. Winkler, M. Wollenhaupt, and T. Baumert, "Real-time observation of transient electron density in water irradiated with tailored femtosecond laser pulses," New J. Phys. **14**, 075021 (2012).
[27] A. Vogel, J. Noack, G. Hüttman, and G. Paltauf, "Mechanisms of femtosecond laser nanosurgery of cells and tissues," Appl. Phys. B **81**(8), 1015–1047 (2005).
[28] A. A. Davis, M. J. Farrar, N. Nishimura, M. M. Jin, and C. B. Schaffer, "Optoporation and genetic manipulation of cells using femtosecond laser pulses," Biophys. J. **105**(4), 862–871 (2013).